Determination of Neutron Flux at the HANARO Cold Neutron Guides

Minyoung Kang[a] , Gwang Min Sun[a], Yuna Lee[a], Sangho Yoo[a] ,Chang- Hee Lee[a], Byung Gun Park[a,b]*
[a]Korea Atomic Energy Research Institute, Daedeok-daero, Yuseong-gu, Daejeon 305-355, Korea
[b]Seoul National University, Shillim-Dong, Gwanak-Gu, Seoul 151-744, Korea
**Email: gmsun@kaeri.re.kr*

1. Introduction

A Cold neutron source (CNS) has been installed at the HANARO research reactor [1]. After the completion of the CNS, it was most important to characterize the neutron beam from the CNS and along the neutron guides. Time-of-Flight (TOF) and gold activation methods were utilized to measure the neutron speed distribution and neutron flux, respectively. In this study, we described the neutron flux monitoring at several positions such as a primary shutter, secondary shutters, and sample or monochromator of the experimental instruments and so on.

2. Method

When ^{197}Au captures a neutron, it undergoes the following nuclear reaction.

$$^{197}Au + n = ^{198}Au + \gamma(411.8\,keV) \quad (1)$$

By measuring the decaying γ-rays from gold, we determine the neutron capture reaction and thermal equivalent neutron flux according to the simple activation formula [2]. Whereas, the real neutron flux(true integrated neutron flux) Φ_R can be deduced from the following procedure. If a wavelength distribution $\Phi(\lambda)$ is well known. Φ_R can be obtained by eq. (2).

$$\phi_R = \int_\lambda \phi(\lambda) d\lambda \quad (2)$$

, where λ is a wave length of neutron. For the case of the neutron beam after monochromator ($\Phi(\lambda)=\Phi_\lambda$, λ is the selected wavelength of neutron after monochromator), Eq. (1) is expressed like,

$$\phi_R = \phi_\lambda = \frac{\sigma_T}{\sigma_\lambda}\phi_T = \frac{\lambda_T}{\lambda}\phi_T \quad (3)$$

, where σ_T, λ_T and Φ_T are capture cross section of ^{197}Au, wave length for the thermal neutron(=1.8 Å when the velocity of neutron is 2200 m/s) and thermal equivalent neutron flux, respectively. For a neutron beam with a continuous wavelength distribution, the neutron capture reaction rate (R) is given as

$$R = \sigma_T \phi_T = \frac{\sigma_T}{\lambda}\frac{\int_\lambda \lambda\phi(\lambda)d\lambda}{\int_\lambda \phi(\lambda)d\lambda}\phi_R \text{, where } \frac{\int_\lambda \lambda\phi(\lambda)d\lambda}{\int_\lambda \phi(\lambda)d\lambda} = \bar{\lambda} \quad (4)$$

, where $\bar{\lambda}$ is an average neutron wavelength. In this study, we determined the $\bar{\lambda}$ from the McStas Monte Carlo simulation [3]. Then, the real neutron flux Φ_R is simply deduced from thermal equivalent neutron flux if we know an average neutron wavelength.

$$\phi_R = \frac{\lambda_T}{\bar{\lambda}}\phi_T \quad (5)$$

3. Measurement

Distributions of the neutron flux at main positions of the cold neutron guide were determined. The measured positions are the primary and secondary shutters of the cold neutron guides, and various neutron scattering instruments. Fig. 1 shows a paper with a gold wire attached to the primary shutter after in-pile guide. The gold wire purchased from Goodfellow company has a diameter of 0.1 mm and its purity is 99.99%.

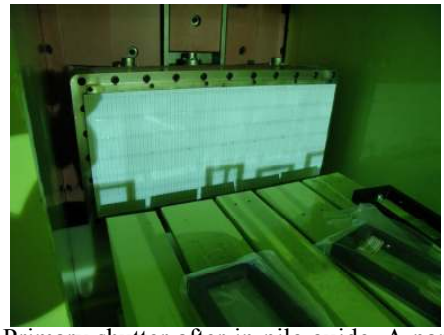

Fig. 1. Primary shutter after in-pile guide. A paper with gold wire is attached to the window surface of the shutter.

The total neutron irradiation time at the primary shutter was 48,600 sec. The activated gold wires were cooled for 3 days before measuring γ-rays. The activated gold wires were measured by using an ORTEC n-type HPGe detector with 40% relative efficiency. The γ-ray spectroscopy system is shown in Fig. 2. Two lead bricks were installed for the collimation of γ-rays from the gold wire.

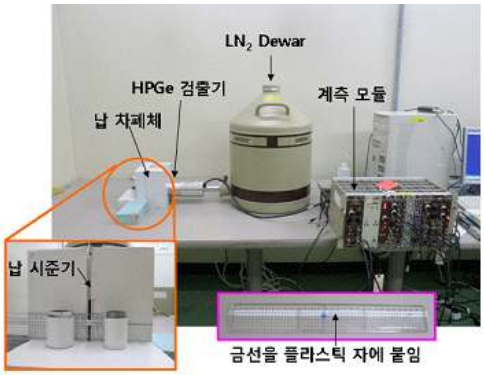

Fig. 2. γ-ray spectroscopy system to measure γ-rays from gold wire.

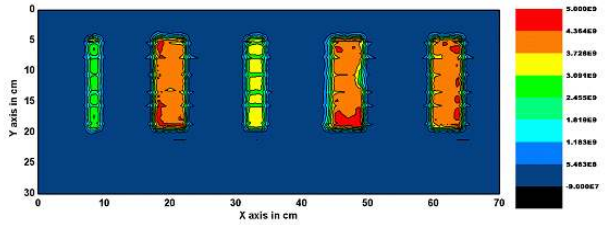

Fig. 3 Contour plot of neutron flux generated by ORIGIN S/W.

4. Results

4.1 distribution of neutron flux at the primary shutter

Fig. 3 shows the spatial distribution of neutron flux at the primary shutter. The maximum flux values of the 5 beam guides are 4.44×10^9, 4.88×10^9, 4.04×10^9 and 4.87×10^9 n/cm^{2}s from the leftmost. Uncertainty of the neutron flux is within ±5% which is propagated from the uncertainty of measurement and detection efficiency.

4.2 Distribution of neutron flux at the secondary shutters

Distributions of neutron flux at the secondary shutters are shown in Fig. 4. The maximum value of the average neutron wavelength calculated from McStas simulation, thermal equivalent neutron flux, real flux at the center of the cross section and maximum value of real flux within the cross section are presented in Table 1. Fig. 5 is distribution of neutron flux at the main location of each neutron scattering device in the cold neutron guide beam and Table 2 lists the neutron fluxes at the various neutron experimental instruments.

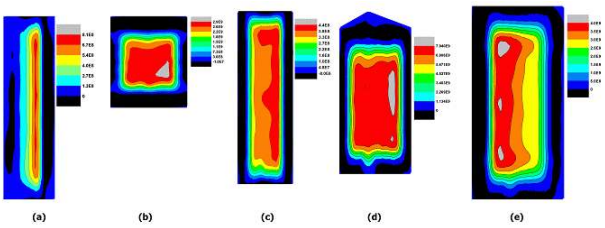

Fig. 4. Neutron flux distribution at CG1 (a), CG2A (b), CG3(c), CG4B(d) and CG5(e).

Table 1. Neutron flux at secondary shutter positions along neutron guides.

Position	$\bar{\lambda}$ [Å]	Φ_T [n/cm^{2}s]	Φ_R [n/cm^{2}s]	Max. Φ_R [n/cm^{2}s]
CG1	5.04	2.01E+09	7.19E+08	1.37E+09
CG2	5.00	5.82E+09	2.10E+09	2.94E+09
CG3	4.30	6.74E+09	2.82E+09	3.56E+09
CG4	5.46	7.71E+09	2.54E+09	2.92E+09
CG5	4.71	8.16E+09	3.11E+09	4.02E+09

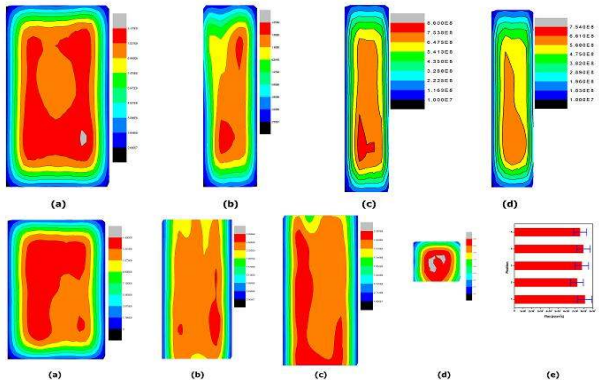

Fig. 5. Neutron flux distribution for up (a) Bio-REF, (b) DC-TOF, (c) GTS, (d) REF-V, below (a) HR-SANS, (b) Cold-TAS(#1), (c) Cold-TAS(#2), (d) 18m-SANS and (e) 40m-SANS.

Table 2. Neutron flux at various neutron scattering instruments.

Position	$\bar{\lambda}$ [Å]	Φ_T [n/cm^{2}s]	Φ_R [n/cm^{2}s]	Max. Φ_R [n/cm^{2}s]
BIO-REF	5.31	2.79E+09	9.46E+08	1.17E+09
DC-TOF	4.22	2.58E+09	1.10E+09	1.47E+09
GTS	5.30	1.83E+09	6.21E+08	8.58E+08
REF-V	5.22	1.49E+09	5.14E+08	7.53E+08
HR-SANS	5.39	3.57E+09	1.19E+09	1.43E+09
Cold-TAS(1)	4.65	5.37E+09	2.08E+09	3.00E+09
Cold-TAS(2)	4.65	3.58E+09	1.39E+09	2.10E+09
18M-SANS	5.19	4.96E+08	1.72E+08	1.82E+09
40M-SANS	5.48	7.76E+07	2.55E+07	2.94E+09

5. Conclusion

Neutron flux and its spatial distribution were determined at the important positions such as primary shutter, secondary shutters and experimental instruments and so on using a gold activation method. These results will be used as one of the checking values of the performance of the CNS, neutron guides and various experimental instruments.

ACKNOWLEDGEMENTS

This work was supported by the National Research Foundation of Korea(NRF) grant funded by the Korea government(MEST).

REFERENCES

[1] Y.K. Kim, K.H. Lee, H.R. Kim, Nuclear Engineering and Design, 238(2008)1664.
[2] Zeev B. Alfassi, Activation Analysis, Vol. I, pp. 40.